POLITECNICO DI TORINO
Repository ISTITUZIONALE

Ultra-efficient degradation of isoquinoline from shale gas wastewater with the diethylamine-ferrate(VI) system: The key role of Fe(IV)/Fe(V) active species

Original
Ultra-efficient degradation of isoquinoline from shale gas wastewater with the diethylamine-ferrate(VI) system: The key role of Fe(IV)/Fe(V) active species / Wang, Y., Chen, X., Chen, L., Cheng, X., Yang, C., Chen, G., Shu, J., Liu, W., Tiraferri, A., Liu, B.. - In: JOURNAL OF HAZARDOUS MATERIALS. - ISSN 0304-3894. - 492:(2025). [10.1016/j.jhazmat.2025.138215]

Availability:
This version is available at: 11583/3000968 since: 2025-06-16T09:05:57Z

Publisher:
Elsevier B.V.

Published
DOI:10.1016/j.jhazmat.2025.138215

Terms of use:

This article is made available under terms and conditions as specified in the corresponding bibliographic description in the repository

Publisher copyright
Elsevier preprint/submitted version

Preprint (submitted version) of an article published in JOURNAL OF HAZARDOUS MATERIALS © 2025, http://doi.org/10.1016/j.jhazmat.2025.138215

(Article begins on next page)

31 October 2026

Removal of organics from shale gas wastewater with the diethylamine-ferrate(VI) system: The key role of Fe(IV)/Fe(V) active species

Ying Wang [a,b], Xin Chen [a,b], Liang Chen [a,b], Xin Cheng [a,b], Chunyan Yang [a,b], Guijing Chen [a,b], Jingyu Shu [a,b], Wen Liu [c], Alberto Tiraferri [d], Baicang Liu [a,b,*]

[a] State Key Laboratory of Hydraulics and Mountain River Engineering, College of Architecture and Environment, Institute for Disaster Management and Reconstruction, Institute of New Energy and Low-Carbon Technology, Sichuan University, Chengdu, Sichuan, 610207, China

[b] Yibin Institute of Industrial Technology, Sichuan University Yibin Park, Section 2, Lingang Ave., Cuiping District, Yibin, Sichuan, 644000, China

[c] The Key Laboratory of Water and Sediment Sciences, Ministry of Education, College of Environmental Sciences and Engineering, Peking University, Beijing 100871, China

[d] Department of Environment, Land and Infrastructure Engineering, Politecnico di Torino, 10129, Turin, Italy

Corresponding author: Baicang Liu, E-mail: bcliu@scu.edu.cn; baicangliu@gmail.com

Abstract

The radical-based advanced oxidation processes currently in use have limited success in treating typical shale gas wastewaters, due to the interference played by background ions and to the formation of potentially toxic disinfection by-products. A novel, non-radical treatment process combining diethylamine (Di) and ferrate, Fe(VI), was investigated in this study. Compared with Fe(VI) alone, the combination with Di provided enhanced performance in degrading various organic pollutants from shale gas wastewater. The measured removal rates were 99.2%, 76.0%, 10.8%, ~100%, and 80.5% for 2,4-di-tert-butylphenol, 6-methylquinoline, tergitolnp-4, indoline, and isoquinoline (IQL), respectively. The degradation rate constant of the Di/Fe(VI) system was almost 3-fold larger than that measured with Fe(VI) alone in the degradation of IQL. A mechanistic investigation suggested that high-valent iron intermediates, namely, Fe(IV)/Fe(V), as well as the ferrate-Di complex, were likely responsible for IQL removal in the Di/Fe(VI) system, while radicals, e.g., $HO^{\bullet}$, $O_2^{\bullet-}$, $^1O_2$, did not play a substantial role. The presence of Di promoted the generation of Fe(IV)/Fe(V) by donating electrons. Increasing Fe(VI) dosage, the Di concentration, and decreasing the pH all enhanced the degradation of IQL. The presence of common ions and different matrix compositions did not considerably affect the removal of IQL. Based on the analytical data and on model calculations, three main, possible reaction pathways for IQL degradation were proposed. The Di/Fe(VI) system was also observed to be reactive against other refractory organics, such as diclofenac, carbamazepine, and ciprofloxacin.

Keywords: Potassium ferrate Fe(VI); Diethylamine; Isoquinoline; Shale gas wastewater (SGW); Active high-valent iron species Fe(IV)/Fe(V).

Main

Shale gas has experienced global development as an alternative to conventional energy sources and to improve the resilience of the energy sector[1]. However, a large amount of shale gas wastewater (SGW) is produced during its extraction activities, posing a threat to the water environments[2–4]. Organic pollutants are the main components of SGW[5], with composition characterized by high variability and complexity[6]. These pollutants are often harmful and carcinogenic, show poor biodegradability and high toxicity[7]. If not properly managed, they may have severe adverse effects for environmental safety and they pose risks of failure for typical treatment technologies deployed to treat SGW, for example, causing membrane fouling and shorter membrane lifespan[8].

Due to the complex composition of SGW, selecting the appropriate treatment train is particularly important. Methods such as biodegradation[9,10], physical treatment [8,11,12], and chemical oxidation[7,13] have been applied. Among them, chemical oxidation is particularly attractive, due to its simplicity and efficiency[14]. However, the chemical oxidation techniques currently used to treat SGW are largely based on radical-driven ($HO^{\bullet}$, $SO_4^{\bullet-}$) advanced oxidation processes. Radicals generally lack selectivity, thus they are susceptible to scavenging reactions by the coexisting background ions in water, e.g., Cl^-, Br^-, HCO_3^-, and tend to produce disinfection by-products[15].

Potassium ferrate (Fe(VI), $Fe^{VI}O_4^{2-}$), has shown potential as an environmentally friendly and multifunctional oxidant with high oxidation capacity and excellent chemical properties[16–18]. The oxidation capacity of Fe(VI) has demonstrated remarkable selectivity, showing resistance to the presence of background impurities in water, thus reducing interference reactions and achieving efficient oxidation of targeted pollutants[19]. The Fe(VI) system can transform organic substances, inorganic substances,

and heavy metal ions, presenting the functions of oxidation, disinfection, and coagulation, simultaneously[20]. However, Fe(VI) has the important limitation of undergoing self-decomposition reactions, arguably the most critical barrier for its implementation in water and wastewater treatment[21]. Appropriate activation techniques are needed to minimize self-decomposition pathways, enhance the oxidation capacity of Fe (VI), and broaden its applicability. As reported in the literature, Fe(IV) and Fe(V) species are generally 2 – 6 orders of magnitude more reactive toward organic compounds than Fe(VI)[22]. As a result, much work has been done to enhance Fe(VI) reactivity to generate Fe(IV)/Fe(V) species through the addition of acids[23], reductants[19,24], metal oxides[18,25,26], metal ions[27,28], silica[29], ammonia[30], carbonaceous materials[16,31], oxidants[32,33], and other activators. For example, the addition of ammonia to Fe(VI) oxidation systems has been shown to improve the overall oxidation efficiency. Organic amines are another family of compounds that can activate Fe(VI) and they happen to be key components in shale gas wastewater, since they are commonly added as acid dispersants/surfactants[3435]. For instance, the amine components of pharmaceuticals are crucial for their oxidation by Fe(VI) in aquatic environments[36,37]. Specifically, during the oxidation of sulfonamides, it is the amine parts that dictate the reaction pathways, leading to the formation of oxidized products[38,39].

In this study, diethylamine (Di) is applied to activate Fe(VI) with the goal of rapid removal of organics in SGW. The specific objectives are: (i) to investigate the removal capacity of various organic pollutants in SGW by combing Di with Fe(VI); (ii) to explore the impact of conditions, including Fe(VI) concentration, Di dosage, solution pH, pollutants concentration, coexisting ions, and water matrix, on the removal performance of pollutants; (iii) to elucidate the presence and role of active species, such as high-valent iron and free radicals; (iv) to propose the possible transformation

pathways of organics in the Di/Fe(VI) system; (v) to assess toxicity changes produced by the organics degradation process; (vi) to preliminarily assess the system for practical applications.

Removal of organic pollutants in SWG by the Di/Fe(VI) system

Oxidation tests based on both the Fe(VI) and the Di/Fe(VI) system were initially performed to transform five compounds typically present in SGW, namely, 2,4-di-tert-butylphenol (2,4-DTB), 6-methylquinoline (6-MQ), tergitolnp-4 (NP), indoline (IDL), and isoquinoline (IQL)) (Fig.1a). The Di/Fe(VI) system outperformed the use of Fe(VI) alone in the removal of all five substances, achieving removal rates of over 70% for the majority of them. IQL was selected for additional, detailed experimentation. The data presented in Fig. 1b suggests that the degradation of IQL was negligible (< 1%) by Di alone within 300 s of reaction. The elimination of 42.5% of IQL was observed with Fe(VI) alone, attributed to the formation of Fe-based species , e.g., Fe(IV) and Fe(V), during the Fe(VI) self-decomposition process[40]. When Di and Fe(VI) were co-added into the reaction solution, the IQL removal was substantially enhanced and reached 80.6% within 300 s of reaction

As illustrated by the data presented in Fig. 1c, the removal of IQL with both the Fe(VI) and the Di/Fe(VI) was only weakly function of the IQL concentration in the range 4.5-10 μM, suggesting an almost pseudo zero-order kinetics under these conditions. The resulting rate constants were 0.029 μM s^{-1} and 0.035 s^{-1}, assuming 0^{th} and 1^{st} order kinetics, respectively, for the Di/Fe(VI) system. Such constants were 3 fold higher than that measured with Fe(VI) alone assuming pseudo 0^{th} order kinetics, namely, 0.011 μM s^{-1}. The results displayed in Fig. 1d indicate that 91.8% and 84.3% residual Fe(VI) was measured in the Fe(VI) and in the Di/Fe(VI) systems, respectively,

suggesting that the overall consumption of Fe(VI) was increased in the Di/Fe(VI) system. In other words, the addition of Di may accelerate the consumption of Fe(VI) and its reactivity, translating into a higher performance of IQL abatement.

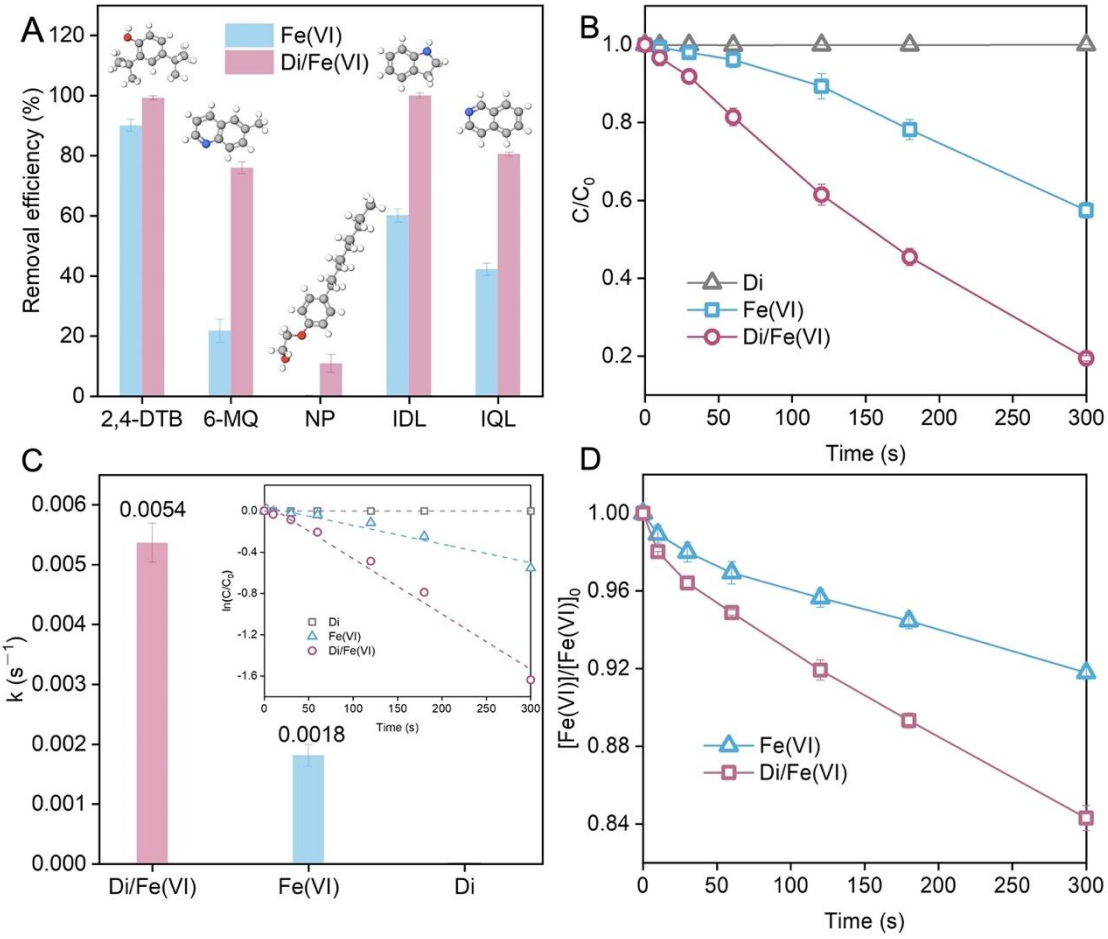


Fig.1. Removal efficiency of 2,4-DTB, 6-MQ, NP-9, IND, and IQL in the Fe(VI) and in the Di/Fe(VI) systems (a); Comparison of the abatement kinetics of IQL in Di alone, Fe(VI) alone, and in the Di/Fe(VI) systems (b); Data fitting with first-order kinetics and resulting rate constants of removal IQL by various systems (c); Residual Fe(VI) concentration as a function of time in the Fe(VI) system and in the Di/Fe(VI) systems (d). In (b) and (d), lines connecting the data points are provided only as a guide for the eye. Unless otherwise stated, the reaction conditions were the following: total reaction time = 300 s; initial contaminant concentration = 10 μM; pH = 9.0; initial reactant concentrations, Fe(VI) = xyz, Di = xyz.

Identification of reactive species

A series of tests was conducted aimed at investigating the possible reactive species contributing to the IQL degradation in the Di/Fe(VI) system, such as hydroxyl radicals ($HO^{\bullet}$), superoxide radicals ($O_2^{\bullet-}$), singlet oxygen ($^1O_2$), the ferrate-Di complex, and/or high-valent iron species (Fe(IV)/Fe(V))[26,31,40–43]. The investigation included radical quenching tests, electron paramagnetic resonance (EPR) spectroscopy, pre-mixed experiments, acquisition of Raman spectra, and assays with probe compounds, such as nitrobenzene (NB) and methyl phenyl sulfoxide (PMSO).

NB was specifically employed to determine the presence and the possible activity of $HO^{\bullet}$ because of its pronounced reactivity with this radical, in contrast with its negligible interaction with other reactive species potentially present in the Di/Fe(VI) system[44,45]. No elimination of NB in the Di/Fe(VI) system was observed (Fig. S2). As indicated by the data plotted in Fig. 2a, the presence of NB had a minor effect on the removal of IQL. Together, these results imply that $HO^{\bullet}$ was likely not involved in the removal of IQL in the Di/Fe(VI) system. The EPR analysis also corroborated this hypothesis, as no DMPO-$HO^{\bullet}$ adduct signal was detected (Fig. 2b). CCl_4 was used as the scavenger for $O_2^{\bullet-}$. Negligible effect on the abatement of IQL was observed in the presence of CCl_4 (Fig. 2a), supporting the contention that $O_2^{\bullet-}$ was also not a key species responsible for IQL removal. This conclusion was further strengthened by the lack of a reduction response of nitro blue tetrazolium (NBT), a characteristic probe for $O_2^{\bullet-}$ (Fig. S3) [46,47]. The potential role of $^1O_2$ in IQL removal was assessed using a system capable of producing $^1O_2$ exclusively, namely, visible light illuminated rose bengal (Vis/RB)[48]. The Vis/RB system did not result in the degradation of IQL (Fig. S4), implying that $^1O_2$ was also not to account for the elimination of IQL. In addition, the

role of ferrate-Di complex was ruled out through the results of pre-mixed experiments (Fig. 2c) and Raman spectroscopy (Fig. 2d).

With the exclusion of $HO^{\bullet}$, $O_2^{\bullet-}$, $^1O_2$, and of the ferrate-Di complex as the reactive species responsible for the elimination of IQL, attention shifted to active iron species, i.e., Fe(IV)/Fe(V). PMSO was used as probe compound to distinguish among different oxidant species through the identification of oxidation products, since Fe(IV)/Fe(V) generally transforms PMSO to the relative sulfone $PMSO_2$ via a direct one or two electron transfer process, while the radical-based oxidation pathway mainly transforms PMSO into other products, such as hydrolyzed PMSO[49–51]. As indicated by the data shown in Fig.2a, the introduction of PMSO markedly slowed down the degradation of IQL in both Fe(VI) and Di/Fe(VI) systems, acting as an important competing substrate. This result indicates that Fe(IV)/Fe(V) may be principally responsible for the IQL degradation. This claim is supported by the findings presented in Figs. 2e and 2f. Full transformation of PMSO to $PMSO_2$ was observed in the two systems, reasonably ruling out the possibility of radical involvement in the Di/Fe(VI) system. The results correlated well with the insights gained from the quenching tests, EPR analysis, and probe compound experiments described above. Additionally, in the presence of Di, the degradation of PMSO and the generation of $PMSO_2$ was significantly faster than that observed in the pure Fe(VI) system. For example, the removal ratio of PMSO at 60 s was 38.5% and 56.5% in the Fe(VI) and in the Di/Fe(VI) system, respectively. The results suggested the role played by Fe(IV) and/or Fe(V) for the enhanced removal rates observed in the Di/Fe(VI) system compared to the Fe(VI) one, the former characterized by stronger oxidation strength[27,52].

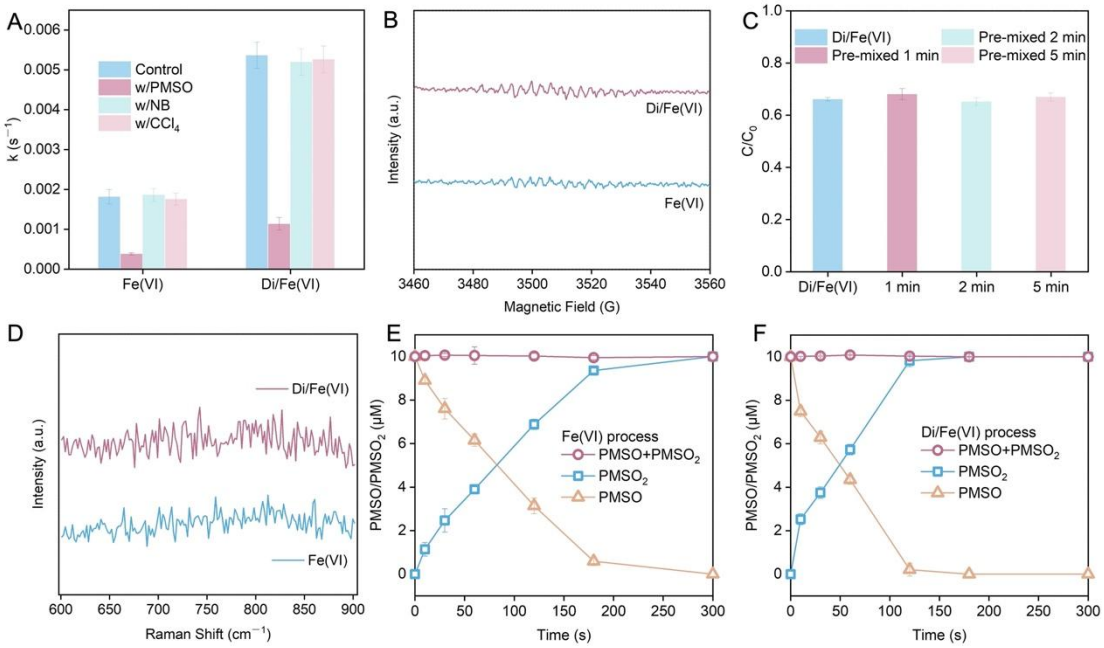


Fig.2. Effect of different scavengers and probes on the removal of IQL in the Fe(VI) and in the Di/Fe(VI) systems (a); EPR detection data of hydroxyl radical ($HO^{\bullet}$) (b); Pre-mixed experiments (c); Raman spectra (d); Degradation of PMSO and generation of $PMSO_2$ in the Fe(VI) (e) and in the Di/Fe(VI) (f) systems. In (e) and (f), lines connecting the data points are provided only as a guide for the eye. Unless otherwise stated, the reaction conditions were the following: total reaction time = 300 s; initial contaminant concentration = 10 μM; pH = 9.0; initial reactant concentrations, Fe(VI) = xyz, Di = xyz.

Insights into the oxidative species

The open circuit potential (OCP) value was measured to evaluate the electron transfer process, hence elucidate the reaction mechanism between Di and Fe(VI). The addition of Fe(VI) led to a significant upward trend in voltage, which may be due to the reduction reaction of Fe(VI) occurring at the electrode (Fig. 3a). After the introduction of Di, there was a downward trend in voltage, indicating a transfer of electrons in the Di/Fe(VI) system. Di may in fact provide electrons to assist in the generation of active

Fe(IV)/Fe(V) from Fe(VI). Fig. 3b illustrates the calculated thermodynamic values for the conversion from Fe(VI) to Fe(IV) (Eq. 1) or Fe(V) (Eq. 2). According to the calculations, the process of converting Fe(VI) to Fe(V) has a free energy barrier (ΔG) value of 155.9 kJ mol^{-1}, which is an endothermic process, while the conversion to Fe(IV) has a ΔG value of −18.03 kJ mol^{-1}, indicating an exothermic process. This result implies that generating Fe(IV) is a favorable step for Fe(VI) oxidation and that Fe(V) may not be directly generated by Di activation of Fe(VI). The possible reaction mechanism of the Di/Fe(VI) system is depicted in Fig. 3c. When Fe(VI) reacts with Di, Fe(IV) may form via a two-electron transfer step. These active high-valent Fe species play roles in removing IQL and can yield Fe(II) (Eq. 3)[40]. The newly formed Fe(II) may react with Fe(VI) to produce Fe(V) (Eq. 4). Fe(V) could then also contribute in the effective degradation of target pollutants and generate Fe(III) (Eq. 5). Moreover, a small portion of Fe(IV) or Fe(V) may also react with Di or undergo self-decomposition, consequently generating Fe(II) or Fe(III), respectively. In conclusion, Di may remarkably promote the decomposition of Fe(VI) to generate more Fe(V) and Fe(IV) via a series of reactions, thus enhancing the degradation efficiency of IQL in the Di/Fe(VI) system.

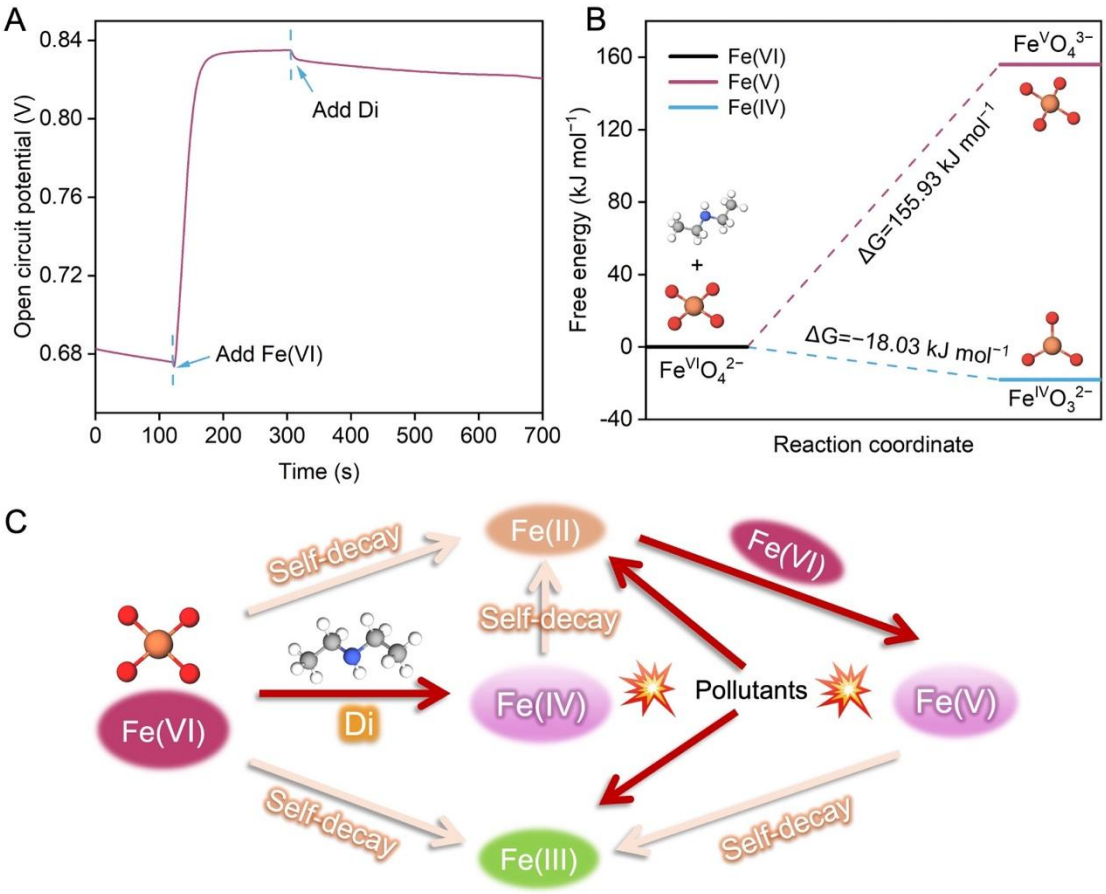
$$Fe(VI) + Di \rightarrow Fe(IV) + Di(O) \quad \text{Eq. 1}$$

$$Fe(VI) + Di \rightarrow Fe(V) + Di^{\bullet+} \quad \text{Eq. 2}$$

$$Fe(IV) + IQL \rightarrow Fe(II) + products \quad \text{Eq. 3}$$

$$Fe(VI) + Fe(II) \rightarrow Fe(V) + Fe(III) \quad \text{Eq. 4}$$

$$Fe(V) + IQL \rightarrow Fe(III) + products \quad \text{Eq. 5}$$



213

214 Fig. 3. Open circuit potential (OCP) measurements (a); ΔG of the transformation of
215 Fe(VI) to Fe(V) and Fe(IV) in the presence of Di (b); Proposed reaction mechanism of
216 the Di/Fe(VI) system (c).

217

218 **Degradation intermediates and pathway of IQL transformation in the Di/Fe(VI)**
219 **system**

220 The reaction intermediate of IQL transformations in the Di/Fe(VI) system were
221 identified using GC-MS. IQL, benzene (TP14), methylbenzene (TP13), ethylbenzene
222 (TP9), o-methylbenzene (TP8), and α-nitrotoluene (TP12) were recognized; the
223 detailed mass spectral information and MS/MS fragmentation patterns are shown in
224 Table S2 and Figs. S5–S10. Based on these identified products, three different possible
225 transformation pathways for the oxidative degradation of IQL by Di/Fe(VI) are

proposed, as shown in Fig. 4d. Although GC-MS can determine measurable intermediate products and help propose possible degradation mechanisms, some short-lived products may not be captured, which impairs the determination of comprehensive pathways. Therefore, we further conducted DFT calculations for IQL.

Active high-valent Fe species exhibit high reactivity with electron-rich organic compounds. The highest occupied molecular orbital (HOMO) of the IQL molecule (Fig. 4b) indicates that electrons can easily escape, making it susceptible to electrophilic attack by high-valent Fe species[53]. To identify the atoms with the highest likelihood of reactivity, the surface electronegativity was analyzed, since this parameter has an impact on the initial affinity with negatively charged Fe(VI)/Fe(V)/Fe(IV). The bar in Fig. 4a illustrates from blue to red color the distribution of positive and negative electrostatic potentials around IQL, with dark areas representing dense positive charges, associated with better affinity for active high-valent Fe species and higher activation chemical potential[54]. To further understand the active sites and degradation pathways of IQL, the Fukui index representing electrophilic attack (f^-) was calculated (Fig. 4c)[55]. Based on the analysis, C4 (f^-=0.0962), C5 (f^-=0.0916), C6 (f^-=0.0952), C7 (f^-=0.0824), C9 (f^-=0.0851), and C10 (f^-=0.0980), may be the most reactive sites, possessing higher f^- values. Generally, electrophilic reagents prefer to attack areas with high negative electrostatic potential[24,56]. It is worth noting that, although the estimated f^- values of C4, C5, and C9 are high, they are of positive electrostatic potentials and are also saturated sites. The benzene ring is inherently a robust structure, where the π electron cloud constitutes an extensive conjugated system that permits a uniform distribution of π electrons throughout the entire ring, thereby imparting enhanced stability[57]. As a result, this configuration is highly resistant to attack by high-valent Fe species. The N1 atom has a high negative electrostatic potential (Fig. 4a), which is another reactive site for

high-valent Fe species attack. Based on these considerations, N1, C6, C7, C10 are proposed as most likely attack sites for high-valent iron species. The bonds cleavage of C6–C10, C10–N1, and N1–C7 are thermodynamically favorable, which may result in the formation of TP1, TP2, and TP3. The bond population of TPs were calculated to corroborate the transformation pathway (Tables S3–S9). A smaller value of bond population means that the bond is weaker and therefore more prone to breakage. In Pathway I, the C4–C7 and C5–C8 bonds in the TP1 are more vulnerable to breakage. The atoms of N1 and C9 are more vulnerable to high-valent iron species attack to produce TP4. As for TP4, the site of N1 is more resistant to electrophilic species attack, while C7–N1, C8–C9, and C2–C7 bonds are weaker. Thus, the generation of TP8 and TP9 may occur. After that, TP8 and TP9 continue to degrade to generate TP13, followed by TP14. Similarly, Pathways II and III were confirmed. The pathways were similar to what discussed in previous studies[58,59].

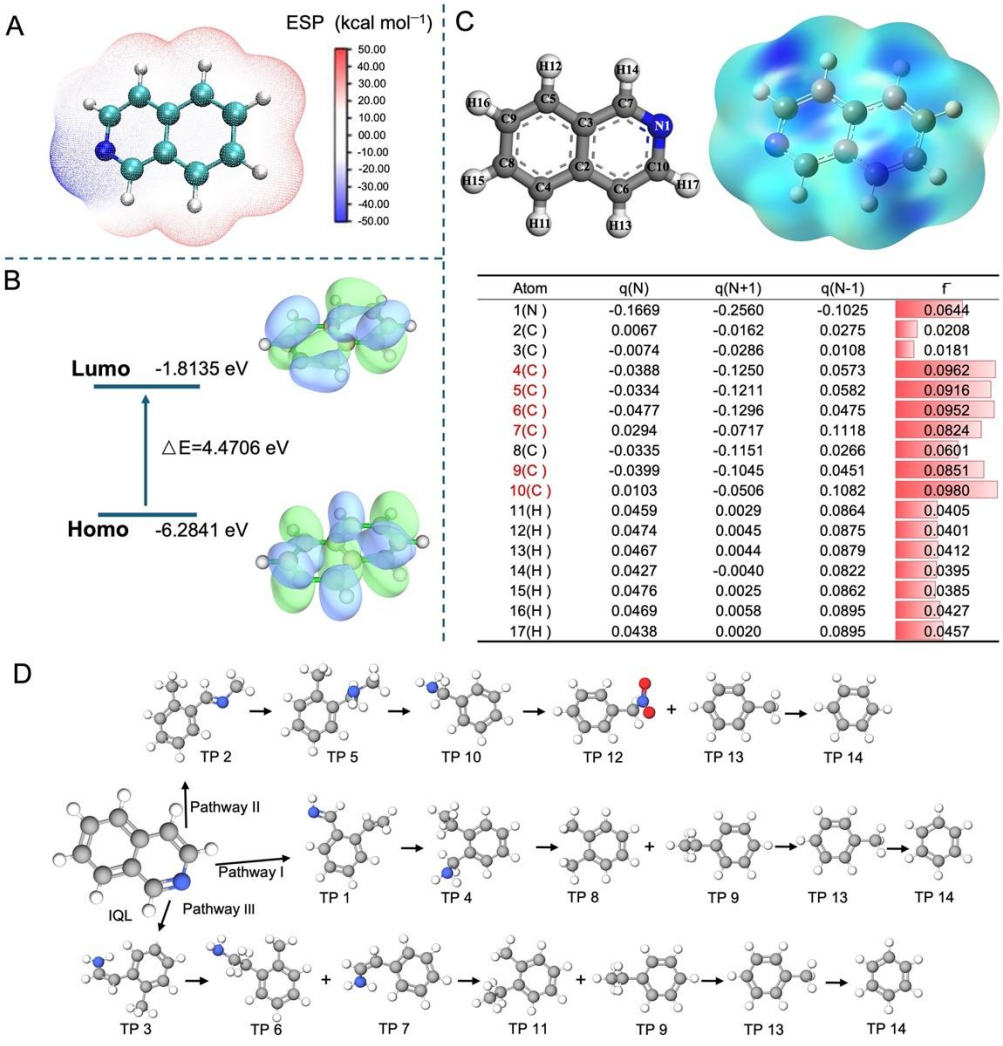


Fig. 4. Electrostatic potential (a), HOMO and LUMO distributions (b), molecular structure and Fukui index (c) of IQL; The proposed mechanisms of IQL degradation in the Di/Fe(VI) system (d).

Toxicity assessment

Acute and chronic toxicity for fish, daphnid, and green algae were predicted by Ecological Structure Activity Relationships (ECOSAR) Predictive Model (Fig. S11). Toxicity for *Daphnia magna*, fathead minnow (*Pimephales promelas*), *Tetrahymena pyriformis*, and oral rat, developmental toxicity, bioaccumulation factors, and mutagenicity values were predicted with the Toxicity Estimation Software Tool (TEST) (Fig. S12). According to the Globally Harmonized System of Classification and

Labeling of Chemical, hazardous chemicals are categorized into four levels: very toxic (LC50/ChV ≤ 1 mg/L), toxic (1 < LC50/ChV ≤ 10 mg/L), harmful (10 < LC50/ChV ≤ 100 mg/L), and not harmful (LC50/ChV > 100 mg/L).

In terms of acute and chronic toxicity prediction by ECOSAR, among the transformation products, TP12 was non-toxic, and most of other TPs had similar toxicity to the parent substance. For *Daphnia magna* , 4 TPs had similar predicted toxicity to the parent substance, while 10 products were identified as more toxic. For fathead minnow, only 1 TP was predicted as toxic, all others as harmful. For *T. pyriformis*, half of the TPs were predicted not harmful, and half as harmful. As for oral rat, almost all TPs exhibited a downward trend of toxicity along the degradation pathway. Overall, the findings suggest the toxicity of most TPs should be lower than that of the parent compound. All the bioaccumulation factors for IQL and TPs were relatively high, indicating a propensity for intracellular accumulation. Five of the TPs exhibited an increase in the bioaccumulation factor, while 7 exhibited a decrease. Note that certain TPs are missing data due to, e.g., complex molecular structures, but these products were relatively harmless to biological and ecological environments[19]. Besides, 11 products were specifically classified in the group “developmental non-toxicity,”. While 4 TPs were found to be mutagenicity positive, 5 TPs were negative. Although the toxicity of these transformation products is not ideal, the strong oxidation behavior of the Di/Fe(VI) system suggests that they may be rapidly mineralized in an appropriately engineered process; see Fig. S13 showing total organic carbon removal as a support for the latter statement.

Effect of conditions on IQL removal in the Di/Fe(VI) system

Oxidant dosage is a significant factor influencing the degradation of contaminants in the chemical oxidation process. The effect of Fe(VI) dosage in the Di/Fe(VI) system

was investigated by oxidizing IQL at different concentration of Fe(VI) (0–600 μM). As illustrated in Fig. 5a, when the dosage of Fe(VI) increased from 0 to 500 μM, the removal of IQL substantially accelerated and the final removal percentages showed a consistent increase from 0% to 80.5% with Fe(VI) concentrations, in tests with duration of 300 s. In contrast, when the Fe(VI) concentration was further increased from 500 μM to 600 μM, the overall removal efficiency showed modest increase (from 80.5% to 84.0%). As the dosage of Fe(VI) increased, more active iron species were produced. However, there seemed to be a critical point above which an increase in Fe(VI) dosage no longer enhanced the degradation efficiency of IQL and instead the reaction became limited by the dosage of Di. Additionally, excessive levels of Fe(VI) may prompt side reactions that promote Fe(VI) consumption[60]. After considering both the efficacy of IQL removal and the costs involved in the process, a concentration of 500 μM Fe(VI) was determined to be the optimal dosage for the Di/Fe(VI) system for the specific conditions considered in this study.

The effect of Di dosage on the elimination of IQL in Di/Fe(VI) system was thus investigated. As depicted in Fig. 5b, when the dosage of Di increased from 0 to 200 μM, the removal of IQL accelerated. However, the overall removal extent did not increase consistently; in detail, the removal extent increased remarkably from roughly 40% to 62% by only increasing Di concentration from 0 to 10 μM, but subsequent step increments from 10 μM to 100 μM only brought about an increase up to ~85% of the overall removal. Actually, a slight decline of IQL removal was observed with further increase of Di dosage to 200 μM. This phenomenon could be attributed to the following reasons: (i) the removal of IQL decreased because of the limiting concentration of Fe(VI); (ii) the addition of excess Di led to the predominance of reactions that resulted in the overall decrease of the concentration of Fe(IV) and Fe(V). Based on the results,

a dosage of 100 μM Di was chosen as the optimal one for the Di/Fe(VI) system under the conditions investigated in this study.

The pH value also stands as an important determinant of the performance of oxidants like Fe(VI) as pointed out, for example, by Tian and colleagues [18]. The findings of the investigation on the effect of pH are graphically depicted in Fig. 5c. When the solution pH was 7.4 and 8.0, there was little or no difference in the final elimination efficiency of IQL within 300 s, with measured removal ratios of around 87.9 % and 88.4%, respectively. However, there was a significant difference when the solution pH was 9.0, at which the reaction rate was notably slower. This deceleration may be attributed to the stability of Fe(VI): as the pH climbs, so does the stability of Fe(VI), resulting in a less reactive state, consistent with the previous studies[18,52,61].

The degradation of IQL by Di/Fe(VI) system at an initial IQL concentration in the range 2 – 40 μM was investigated (Fig. 5d). An overall lower removal efficacy was observed with an increasing amount of IQL. Note that these data also allow expanding the discussion around reaction kinetics compared to that mentioned above. The kinetics rate did increase slightly with IQL concentration in the low spectrum of concentrations, implying a weak 1^{st} order rate. The resulting 1^{st} rate constant was 0.0052 s^{-1} in the range 0 to ~5 μM of IQL. Above this point, the kinetics rate quickly became nearly constant with IQL concentration, or did not show an obvious trend, and may be described by a 0^{th} order constant equal to 0.039 μM s^{-1}. Note that this result is consistent with the above discussion about kinetics based on the data presented in Fig. 1C. Indeed, such 0^{th} order constant extracted from a concentration range between 0 and 40 μM of IQL is similar to that presented above and based only on the test performed with initial IQL concentration of 10 μM. As of now, it is not clear whether the observed slowing down of kinetics is due to an inhibitory effect of IQL substrate at high concentrations, and/or

to an insufficient reactant/substrate ratio under such conditions. Overall, this kinetics behavior translates into a lower relative removal efficiency at any fixed time when starting from higher contaminant concentrations, and it suggest that the reaction time required to achieve a certain removal efficiency may increase considerably with the initial IQL concentration.

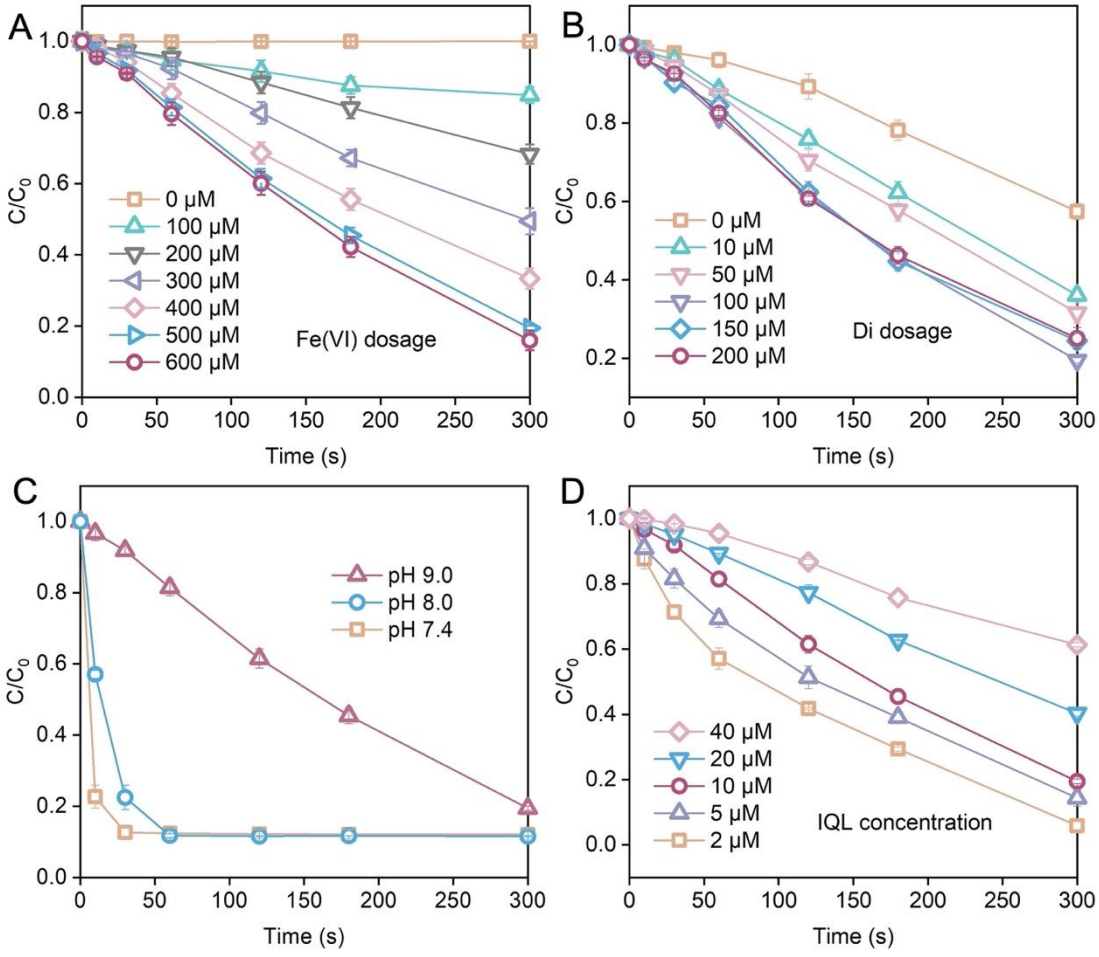


Fig. 5. Effect of Fe(VI) dosage(a), Di dosage (b), solution pH (c), and IQL concentration (d) on the relative removal efficiency of IQL by Di/Fe(VI) system, plotted as a function of reaction time. Lines connecting the data points are provided only as a guide for the eye. Unless otherwise stated, the reaction conditions were the following: initial contaminant concentration = 10 μM; pH = 9.0; initial reactant concentrations, Fe(VI) = xyz, Di = xyz.

Considerations for practical application of the Di/Fe(VI) system

Several common ions typically present in shale gas wastewater matrices (Br^-, Cl^-, F^-, HCO_3^-, NO_3^-, SO_4^{2-}, Na^+, K^+, Ca^{2+}, and Mg^{2+})[62] were investigated to evaluate their effects on the oxidation performance of the Di/Fe(VI) system. As presented in Fig. 6a, the presence of Br^- had a slight effect on the removal of IQL. As the Br^- concentration gradually increased, the removal rate of IQL gradually decreased. When the concentration of Br^- was 0.5 mM and 1.0 mM, the removal efficiency of IQL decreased to 74.7% and 71.3%, respectively. This result may be explained with the help of a previous study by Li and colleagues[45], who explored the formation of bromate (BrO_3^-) in the co-presence of Fe(VI) and Br^-, the study suggesting that the formation of BrO_3^- was due to the oxidation of OBr^- by Fe(VI) and Fe(V)/Fe(IV), which may have thus reduced the production and availability of Fe(IV)/Fe(V) for IQL removal. Apart from Br^-, the presence of the other ions at concentrations of 0.5 and 1.0 mM did not demonstrate substantial inhibitory effects. Overall, the removal efficiencies were always above 70%, despite the presence of potentially competing ions, which may be considered a largely inconsequential effect of ion composition at least in concentrations equal or below 1 mM, pointing out the potential of this system for a more selective oxidation strategy compared to current options.

To assess the feasibility of the Di/Fe(VI) system in different water matrices, experiments were also conducted using SGW, tap water, ultrapure water, and river water. As shown in Fig. 6b, IQL removal in ultrapure water, tap water, and water from the Jiangan river water were practically the same, while the test performed in SGW showed a minor inhibition role on IQL removal, maybe due to the presence of complex organic substances, which may compete with IQL for Fe(VI)[5]. Finally, the oxidation performance of the Di/Fe(VI) system was also preliminarily tested for the removal of

other pollutants, including DCF, CBZ, CIP, SMX, and 4-CP. As presented in Fig. 6c, the removal efficiencies were all higher than 80% within 300 s of experiment.

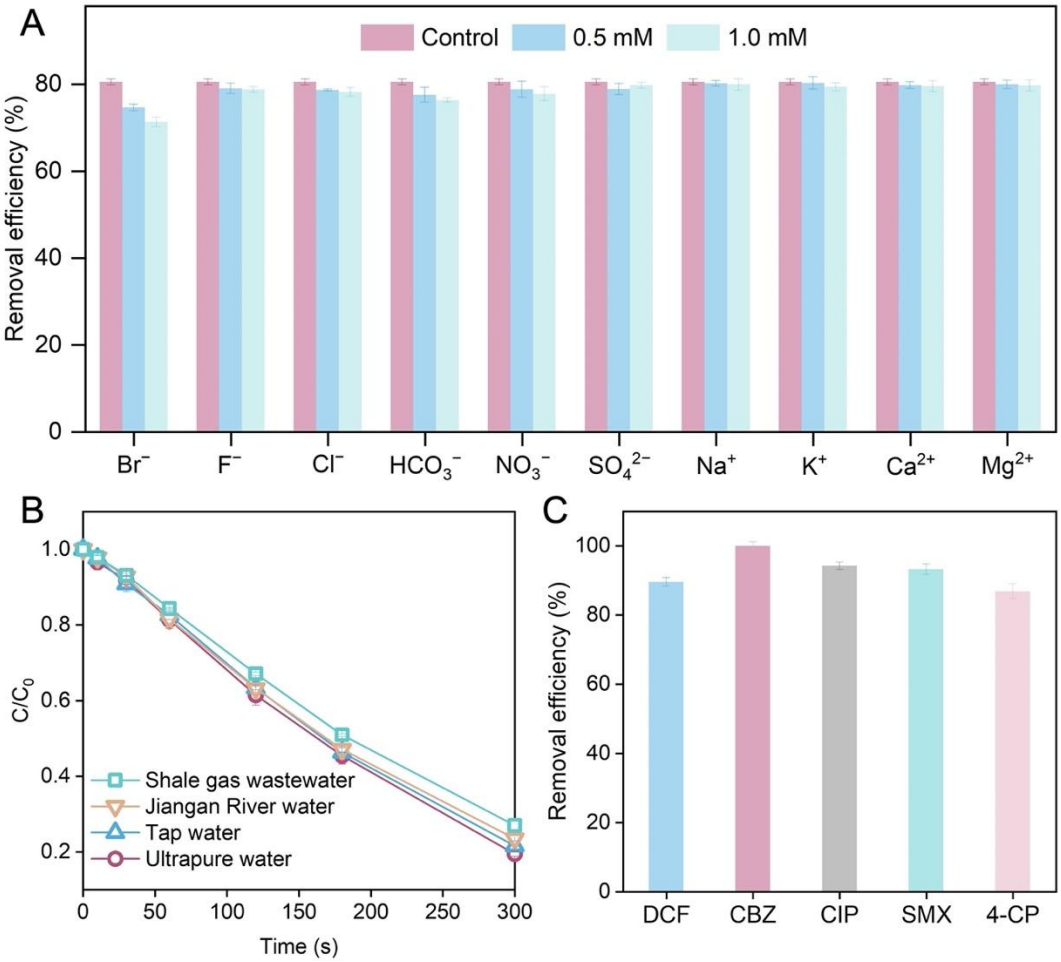


Fig. 6. Effect on the IQL removal performance in the Di/Fe(VI) system of the presence of F^-, Br^-, Cl^-, HCO_3^-, NO_3^-, SO_4^{2-}, Na^+, K^+, Ca^{2+}, and Mg^{2+} (a), of the water matrix (b). In (b), lines connecting the data points are provided only as a guide for the eye. Removal efficiency of diclofenac (DCF), carbamazepine (CBZ), ciprofloxacin (CIP), sulfamethoxazole (SMX), and 4-chlorophenol (4-CP) in Di/Fe(VI) system (c). Unless otherwise stated, the reaction conditions were the following: total reaction time = 300 s; initial contaminant concentration = 10 μM; pH = 9.0; initial reactant concentrations, Fe(VI) = xyz, Di = xyz.

Conclusions

In this study, diethylamine was observed to be an efficient activator of Fe(VI) to enhance the removal of organic pollutants in shale gas wastewater. Under conditions consisting of pH value equal to 9.0, Fe(VI) dosage of 500 μM, Di dosage of 100 μM, and initial isoquinoline (IQL) concentration of 10 μM, the degradation rate reached 80.6% within 300 s. The degradation of IQL in the Fe(VI) and in the Di/Fe(VI) systems was found to fit a pseudo first-order kinetic model at low contaminant concentration and near zero-order kinetics at concentrations > ~5 μM, with the rate constant observed in Di/Fe(VI) system almost 3 fold larger than that measured with Fe(VI) alone. Fe(IV) and Fe(V) were identified as the primary active species for IQL removal in the Di/Fe(VI) system, and the presence of Di promoted the generation of Fe(IV)/Fe(V). Based on the intermediates identified with GC-MS measurements and density functional theory calculations (Fukui indices and bond populations), three oxidation pathways of IQL by Di/Fe(VI) were proposed. The results of coexisting ions and water matrix indicated no substantial effect of water composition for ionic concentrations ≤ 1 mM, suggesting that the Di/Fe(VI) system is a potentially stable and effective treatment method even for matrices with complex inorganic composition. The Di/Fe(VI) system was also effective in the removal of other organic molecules, namely, diclofenac, carbamazepine, ciprofloxacin, sulfamethoxazole, and 4-chlorophenol, implying a wide range of applicability.

Methods

Chemicals and reagents

In this work, potassium ferrate (K_2FeO_4, Fe(VI)) was synthesized based on a wet chemical oxidation method according to Thompsons' study [63]; relevant information is given in Text S1 of the Supporting Information (SI). Shale gas wastewater was sourced

427 from Nanchuan, Chongqing. Detailed descriptions of the chemicals and reagents are
428 provided in Text S2.
429 Experimental procedures
430 All experiments were conducted in 150 mL glass beaker containing 100 mL
431 reaction solution and initiated by simultaneously adding the specific amount of Di and
432 solid Fe(VI) while stirring at 300 r min^{-1} with a magnetic stirrer. Unless otherwise
433 specified, solution pH was maintained at pH 9.0 by addition of 10 mM borate buffer,
434 and the fluctuation of reaction pH was controlled in ± 0.5 units. As needed, additional
435 acid or alkali was added to adjust the solution pH. At scheduled time interval, an aliquot
436 of 1 mL solution was sampled and mixed with excess $NH_2OH{\cdot}HCl$ to terminate the
437 reactions (Huang et al., 2021; Wang et al., 2023). Then, the samples were filtered
438 through a 0.22 μm PTFE membrane into 2 mL vials before analysis. All the oxidation
439 experiments were independently repeated at least twice, and the obtained average
440 values and related standard deviations are presented. Pre-mixed experimental
441 procedures are described in Text S3.
442 Analytical methods
443 The pH value of the solution was determined with a regularly calibrated pH meter
444 (Mettler Toledo FE-28, USA). The concentrations of pollutants (e.g., 2,4-DTB, 6-MQ,
445 NP, IDL, IQL, NB, PMSO, and $PMSO_2$) were monitored with a ultra-performance
446 liquid chromatography apparatus (Shimadzu LC-16, Japan), equipped with a UV
447 detector and Shim-pack GIST C18 (5 μm, 4.6 × 250 mm); additional details are
448 summarized in Text S4 and Table S1. Absorbance measurement were conducted with a
449 AquaMate 8000 UV−vis spectrometer (USA). The desired Fe(VI) concentrations were
450 quantified at a wavelength of 510 nm with a molar absorption coefficient of $\varepsilon_{510\,nm}$ =
451 1150 M^{-1} cm^{-1} [64]. Detailed experimental procedures for measuring residual Fe(VI) are

presented in Text S5. Other analytical methods are described in Texts S6–S12.

Density functional theory calculations

To predict the most likely active reaction sites of IQL, DFT calculations were performed via Gaussian software. The IQL geometry optimization was conducted using the Gaussian 16 software with the B3LYP-D3/6–311+G(d) method. Detailed information is presented in Text S13.

Data availability

All data are presented in the article and its Supplementary Information. Source data are provided with this paper.

References

1. Kerr, R. A. Natural Gas From Shale Bursts Onto the Scene. *Science* **328**, 1624–1626 (2010).

2. Bonetti, P., Leuz, C. & Michelon, G. Large-sample evidence on the impact of unconventional oil and gas development on surface waters. *Science* **373**, 896–902 (2021).

3. Vidic, R. D., Brantley, S. L., Vandenbossche, J. M., Yoxtheimer, D. & Abad, J. D. Impact of Shale Gas Development on Regional Water Quality. *Science* **340**, 1235009 (2013).

4. Yang, H., Flower, R. J. & Thompson, J. R. Shale-Gas Plans Threaten China's Water Resources. *Science* **340**, 1288–1288 (2013).

5. Butkovskyi, A., Bruning, H., Kools, S. A. E., Rijnaarts, H. H. M. & Van Wezel, A. P. Organic Pollutants in Shale Gas Flowback and Produced Waters: Identification, Potential Ecological Impact, and Implications for Treatment Strategies. *Environ. Sci. Technol.* **51**, 4740–4754 (2017).

6. Tao, Z., Liu, C., He, Q., Chang, H. & Ma, J. Detection and treatment of organic matters in hydraulic fracturing wastewater from shale gas extraction: A critical review. *Sci. Total Environ.* **824**, 153887 (2022).

7. Chen, X., Zhao, G., Yang, Z. & Li, Q. Molecular comparison of organic matter removal from shale gas flowback wastewater: Ozonation versus Fenton process. *Sci. Total Environ.* **905**, 167147 (2023).

8. Liu, Y. *et al.* Green aerogel adsorbent for removal of organic compounds in shale gas wastewater: High-performance tuning and adsorption mechanism. *Chem. Eng. J.* **416**, 129100 (2021).

9. Hanson, A. J. *et al.* High total dissolved solids in shale gas wastewater inhibit

488 biodegradation of alkyl and nonylphenol ethoxylate surfactants. *Sci. Total Environ.* **668**,
489 1094–1103 (2019).
490 10. Sun, Y., Huang, L., Lai, C., Li, H. & Yang, P. Removal of organics from shale gas
491 fracturing flowback fluid using expanded granular sludge bed and moving bed biofilm
492 reactor. *Environ. Technol.* **42**, 3736–3746 (2021).
493 11. Wang, B., Xiong, M., Shi, B., Li, Z. & Zhang, H. Treatment of shale gas flowback
494 water by adsorption on carbon- nanotube-nested diatomite adsorbent. *J. Water Process*
495 *Eng.* **42**, 102074 (2021).
496 12. Ye, J. *et al.* Removal of 6-methylquinoline from shale gas wastewater using
497 electrochemical carbon nanotubes filter. *Chemosphere* **359**, 142259 (2024).
498 13. Tang, P. *et al.* Organics removal from shale gas wastewater by pre-oxidation
499 combined with biologically active filtration. *Water Res.* **196**, 117041 (2021).
500 14. Tan, B., He, Z., Fang, Y. & Zhu, L. Removal of organic pollutants in shale gas
501 fracturing flowback and produced water: A review. *Sci. Total Environ.* **883**, 163478
502 (2023).
503 15. Lee, J., Gunten, U. V. & Kim, J. H. Persulfate-based Advanced Oxidation: Critical
504 Assessment of Opportunities and Roadblocks. *Environ. Sci. Technol.* **54**, 3064–3081
505 (2020).
506 16. Deng, Z. *et al.* Highly efficient activation of ferrate (VI) via corncob biochar
507 assisted by electrochemistry for the removal of sulfamethoxazole from water. *Chem.*
508 *Eng. J.* **484**, 149479 (2024).
509 17. Liu, M. *et al.* Insights into manganese(VII) enhanced oxidation of benzophenone-
510 8 by ferrate(VI): Mechanism and transformation products. *Water Res.* **238**, 120034
511 (2023).
512 18. Tian, B., Wu, N., Liu, M., Wang, Z. & Qu, R. Promoting Effect of Silver Oxide

513 Nanoparticles on the Oxidation of Bisphenol B by Ferrate(VI). *Environ. Sci. Technol.*
514 **57**, 15715–15724 (2023).
515 19. Chen, K. *et al.* New insights into degradation of emerging contaminants by
516 S(IV)/Fe(VI) system in neutral water: Performance enhancement, reaction mechanisms
517 and toxicity assessment. *Sep. Purif. Technol.* **328**, 125112 (2024).
518 20. Wang, J. *et al.* Oxidation of selected fluoroquinolones by ferrate(VI) in water:
519 Kinetics, mechanism, effects of constituents, and reaction pathways. *Environ. Res.* **243**,
520 117845 (2024).
521 21. Deng, Y. & Abdel-Shafy, H. I. Barriers to Ferrate(VI) Application in Water and
522 Wastewater Treatment. *Environ. Sci. Technol.* **58**, 3057–3060 (2024).
523 22. Sharma, V. K. *et al.* Reactive High-Valent Iron Intermediates in Enhancing
524 Treatment of Water by Ferrate. *Environ. Sci. Technol.* **56**, 30–47 (2022).
525 23. Manoli, K. *et al.* Pharmaceuticals and pesticides in secondary effluent wastewater:
526 Identification and enhanced removal by acid-activated ferrate(VI). *Water Res.* **148**,
527 272–280 (2019).
528 24. Zhao, Z. *et al.* New insights into the Ferrate-Sulfite system for the degradation of
529 polycyclic aromatic Hydrocarbons: A dual role for sulfite. *Chem. Eng. J.* **477**, 147157
530 (2023).
531 25. Shu, J. *et al.* Insight into the mechanism of ferrate(VI) activation by mineral zincite
532 for carbamazepine degradation: Role of Fe(V) species and free radical induction. *Chem.*
533 *Eng. J.* **473**, 145360 (2023).
534 26. Wu, Y. *et al.* Enhanced Oxidation of Organic Compounds by the Ferrihydrite–
535 Ferrate System: The Role of Intramolecular Electron Transfer and Intermediate Iron
536 Species. *Environ. Sci. Technol.* (2023) doi:10.1021/acs.est.3c05798.
537 27. Feng, M., Jinadatha, C., McDonald, T. J. & Sharma, V. K. Accelerated Oxidation

of Organic Contaminants by Ferrate(VI): The Overlooked Role of Reducing Additives. *Environ. Sci. Technol.* **52**, 11319–11327 (2018).

28. Zhang, X. *et al.* Effect of Metal Ions on Oxidation of Micropollutants by Ferrate(VI): Enhancing Role of FeIV Species. *Environ. Sci. Technol.* **55**, 623–633 (2021).

29. Manoli, K., Nakhla, G., Feng, M., Sharma, V. K. & Ray, A. K. Silica gel-enhanced oxidation of caffeine by ferrate(VI). *Chem. Eng. J.* **330**, 987–994 (2017).

30. Rougé, V., Nguyen, P. T. T. H., Allard, S. & Lee, Y. Reaction of Amino Acids with Ferrate(VI): Impact of the Carboxylic Group on the Primary Amine Oxidation Kinetics and Mechanism. *Environ. Sci. Technol.* acs.est.2c03319 (2022) doi:10.1021/acs.est.2c03319.

31. Wang, Y. *et al.* Enhanced ferrate(VI) oxidation of organic pollutants through direct electron transfer. *Water Res.* **244**, 120506 (2023).

32. Niu, L. *et al.* Ferrate(VI)/Periodate System: Synergistic and Rapid Oxidation of Micropollutants via Periodate/Iodate-Modulated Fe(IV)/Fe(V) Intermediates. *Environ. Sci. Technol.* (2023) doi:10.1021/acs.est.2c08965.

33. Wang, Z. *et al.* Ferrate(VI)/percarbonate for the oxidation of micropollutants: Interactive activation and release of low-concentration hydrogen peroxide for efficient electron utilization. *J. Hazard. Mater.* **469**, 134029 (2024).

34. Thacker, J. B., Carlton, D. D., Hildenbrand, Z. L., Kadjo, A. F. & Schug, K. A. Chemical Analysis of Wastewater from Unconventional Drilling Operations. *Water* **7**, 1568–1579 (2015).

35. Baum, J. C., Feng, M., Guo, B., Huang, C.-H. & Sharma, V. K. Generation of Iron(IV) in the Oxidation of Amines by Ferrate(VI): Theoretical Insight and Implications in Oxidizing Pharmaceuticals. *ACS EST Water* **1**, 1932–1940 (2021).

563 36. Liu, H. *et al.* Oxidative degradation of chlorpyrifos using ferrate(VI): Kinetics and
564 reaction mechanism. *Ecotoxicol. Environ. Saf.* **170**, 259–266 (2019).
565 37. Luo, C., Feng, M., Sharma, V. K. & Huang, C.-H. Oxidation of Pharmaceuticals
566 by Ferrate(VI) in Hydrolyzed Urine: Effects of Major Inorganic Constituents. *Environ.*
567 *Sci. Technol.* **53**, 5272–5281 (2019).
568 38. Feng, M. *et al.* Oxidation of Sulfonamide Antibiotics of Six-Membered
569 Heterocyclic Moiety by Ferrate(VI): Kinetics and Mechanistic Insight into SO2
570 Extrusion. *Environ. Sci. Technol.* **53**, 2695–2704 (2019).
571 39. Kim, C. *et al.* Ferrate promoted oxidative cleavage of sulfonamides: Kinetics and
572 product formation under acidic conditions. *Chem. Eng. J.* **279**, 307–316 (2015).
573 40. Zhang, H. *et al.* Enhanced ferrate(VI)) oxidation of sulfamethoxazole in water by
574 CaO2: The role of Fe(IV) and Fe(V). *J. Hazard. Mater.* **425**, 128045 (2022).
575 41. Luo, M. *et al.* Efficient activation of ferrate(VI) by colloid manganese dioxide:
576 Comprehensive elucidation of the surface-promoted mechanism. *Water Res.* **215**,
577 118243 (2022).
578 42. Tian, S.-Q., Wang, L., Liu, Y.-L. & Ma, J. Degradation of organic pollutants by
579 ferrate/biochar: Enhanced formation of strong intermediate oxidative iron species.
580 *Water Res.* **183**, 116054 (2020).
581 43. Yang, T. *et al.* UVA-LED-Assisted Activation of the Ferrate(VI) Process for
582 Enhanced Micropollutant Degradation: Important Role of Ferrate(IV) and Ferrate(V).
583 *Environ. Sci. Technol.* **56**, 1221–1232 (2022).
584 44. Lei, Y. *et al.* Assessing the Use of Probes and Quenchers for Understanding the
585 Reactive Species in Advanced Oxidation Processes. *Environ. Sci. Technol.* **57**, 5433–
586 5444 (2023).
587 45. Li, G. *et al.* Enhancing Ferrate Oxidation of Micropollutants via Inducing

588 Fe(V)/Fe(IV) Formation Needs Caution: Increased Conversion of Bromide to Bromate.
589 *Environ. Sci. Technol.* acs.est.3c01395 (2023) doi:10.1021/acs.est.3c01395.
590 46. Cheng, C., Chen, L., Chou, C. & Liang, J. Investigations of riboflavin photolysis
591 via coloured light in the nitro blue tetrazolium assay for superoxide dismutase activity.
592 *J. Photochem. Photobiol. B* **148**, 262–267 (2015).
593 47. Kono, Y. Reprint of: Generation of Superoxide Radical during Autoxidation of
594 Hydroxylamine and an Assay for Superoxide Dismutase. *Arch. Biochem. Biophys.* **726**,
595 109247 (2022).
596 48. Lee, H., Lee, C. & Kim, J.-H. Response to Comment on "Activation of Persulfate
597 by Graphitized Nanodiamonds for Removal of Organic Compounds". *Environ. Sci.*
598 *Technol.* **51**, 5353–5354 (2017).
599 49. Huang, Z.-S. *et al.* Ferrate self-decomposition in water is also a self-activation
600 process: Role of Fe(V) species and enhancement with Fe(III) in methyl phenyl
601 sulfoxide oxidation by excess ferrate. *Water Res.* **197**, 117094 (2021).
602 50. Luo, C., Feng, M., Zhang, T., Sharma, V. K. & Huang, C.-H. Ferrate(VI) Oxidation
603 of Pharmaceuticals in Hydrolyzed Urine: Enhancement by Creatinine and the Role of
604 Fe(IV). *ACS EST Water* **1**, 969–979 (2021).
605 51. Sun, S. *et al.* Activation of ferrate by carbon nanotube for enhanced degradation of
606 bromophenols: Kinetics, products, and involvement of Fe(V)/Fe(IV). *Water Res.* **156**,
607 1–8 (2019).
608 52. Huang, Z.-S. *et al.* Impact of Phosphate on Ferrate Oxidation of Organic
609 Compounds: An Underestimated Oxidant. *Environ. Sci. Technol.* **52**, 13897–13907
610 (2018).
611 53. Qi, X. *et al.* Ferrate(VI) oxidation of substituted nitrobenzene compounds: Kinetics,
612 degradation, and oxidized products. *Chem. Eng. J.* **488**, 150921 (2024).

54. Zhang, H. *et al.* Different reaction mechanisms of SO4•− and •OH with organic compound interpreted at molecular orbital level in Co(II)/peroxymonosulfate catalytic activation system. *Water Res.* **229**, 119392 (2023).

55. Yang, C. *et al.* One-step synthesis of a 3D/2D Bi2WO6/g-C3N4 heterojunction for effective photocatalytic degradation of atrazine: Kinetics, degradation mechanisms and ecotoxicity. *Sep. Purif. Technol.* **288**, 120609 (2022).

56. Chen, X.-J. *et al.* pH-Driven Efficacy of the Ferrate(VI)–Peracetic Acid System in Swift Sulfonamide Antibiotic Degradation: A Deep Dive into Active Species Evolution and Mechanistic Insights. *Environ. Sci. Technol.* **57**, 20206–20218 (2023).

57. Deng, S. *et al.* Unveiling the activation mechanism: The role of nitrogen-doped biochar in enhancing Fe(VI) catalysis. *Chem. Eng. J.* **486**, 150263 (2024).

58. He, F., Wang, J., Li, Y. & Sun, H. Quantum Chemistry Calculations on the Mechanism of Isoquinoline Ring-Opening and Denitrogenation in Supercritical Water. *Ind. Eng. Chem. Res.* **56**, 1782–1790 (2017).

59. Ogunsola, O. M. Decomposition of isoquinoline and quinoline by supercritical water. *J. Hazard. Mater.* **74**, 187–195 (2000).

60. Zhang, Z. *et al.* Combining ferrate(VI) with thiosulfate to oxidize chloramphenicol: Influencing factors and degradation mechanism. *J. Environ. Chem. Eng.* **9**, 104625 (2021).

61. Graham, N., Jiang, C., Li, X.-Z., Jiang, J.-Q. & Ma, J. The influence of pH on the degradation of phenol and chlorophenols by potassium ferrate. *Chemosphere* **56**, 949–956 (2004).

62. Xie, W. *et al.* Shale gas wastewater characterization: Comprehensive detection, evaluation of valuable metals, and environmental risks of heavy metals and radionuclides. *Water Res.* **220**, 118703 (2022).

638 63. Thompson, G. W., Ockerman, L. T. & Schreyer, J. M. Preparation and Purification
639 of Potassium Ferrate. VI. *J. Am. Chem. Soc.* **73**, 1379–1381 (1951).
640 64. Guo, B. *et al.* Enhanced Oxidation of Antibiotics by Ferrate Mediated with Natural
641 Organic Matter: Role of Phenolic Moieties. *Environ. Sci. Technol.* acs.est.3c03165
642 (2023) doi:10.1021/acs.est.3c03165.
643

Acknowledgments

This work was supported by the National Natural Science Foundation of China (52070134, 52270075, 52300101), Sichuan University and Zigong City People's Government Strategic Cooperation Project (2022CDZG-7), Litree Purifying Technology Co., Ltd. Project (2021H012), and Sichuan University and Yibin City People's Government strategic cooperation project (2020CDYB-2). A.T. acknowledges the support of Politecnico di Torino. We would like to thank the Institute of New Energy and Low-Carbon Technology, Sichuan University, for Raman tests. We would like to thank the Analytical & Testing Center of Sichuan University for EPR measurement.

Author information

Authors and Affiliations

State Key Laboratory of Hydraulics and Mountain River Engineering, College of Architecture and Environment, Institute for Disaster Management and Reconstruction, Institute of New Energy and Low-Carbon Technology, Sichuan University, Chengdu, Sichuan, 610207, China; Yibin Institute of Industrial Technology, Sichuan University Yibin Park, Section 2, Lingang Ave., Cuiping District, Yibin, Sichuan, 644000, China

Ying Wang, Xin Chen, Liang Chen, Xin Cheng, Chunyan Yang, Guijing Chen, Jingyu Shu & Baicang Liu

The Key Laboratory of Water and Sediment Sciences, Ministry of Education, College of Environmental Sciences and Engineering, Peking University, Beijing 100871, China

Wen Liu

Department of Environment, Land and Infrastructure Engineering, Politecnico di Torino, 10129, Turin, Italy

Alberto Tiraferri

Contributions

Ying Wang: Methodology, Investigation, Formal analysis, Writing – original draft. Xin Chen: Data Curation, Software. Liang Chen: Software. Xin Cheng: Visualization, Investigation. Chunyan Yang: Visualization, Investigation. Guijing Chen: Methodology, Software. Jingyu Shu: Software. Wen Liu: Software. Alberto Tiraferri: Writing – review & editing. Baicang Liu: Conceptualization, Supervision, Writing – review & editing.

Corresponding author

Correspondence to Baicang Liu

Ethics declarations

The authors declare that they have no known competing financial interests or personal relationships that could have appeared to influence the work reported in this paper.